Journal of Radiation and Nuclear Applications
*An International Journal*

http://dx.doi.org/10.18576/jrna/060304

# Tracting and Studying the Leaching of Uranium, Thorium and REE from Microgranite at the South Eastern Part of Wadi Baroud, North Eastern Desert, Egypt

*Neveen S. Abed, Mahmoud S. Khalafalla, M. Abdel Monseif, Mahmoud R. Khattab*[*]

Nuclear Materials Authority (NMA), P.O. Box 530, El-Maadi, Cairo, Egypt.

Received: 15 July. 2021, Revised: 22 July. 2021, Accepted: 24 July. 2021.

**Abstract:** Egypt needs to provide large quantities of nuclear fuel, after its decision to build a number of nuclear plants that will run on nuclear fuel. Uranium is the most important nuclear fuel and has been utilized for producing electrical energy without the threat of global warming. South Eastern Part of Wadi Baroud is located in the Northern Eastern Desert of Egypt at about 20 km westward Safaga City. The purpose of this study was to investigate the mineralogical content of South Eastern part of Wadi Baroud microgranite which revealed that the main mineral associations were represented by uranium, thorium and rare earth elements (REEs)-minerals. Also to investigate the process of sulphuric acid leaching of a representative samples from a new ore of uranium occurrence in South Eastern Part of Wadi Baroud. From the acidic atmospheric agitation leaching study upon the dissolution of U, Th and REEs from the study ore material, it can be concluded that this leaching method is satisfactory in dissolving 97.6 %, 98.8 % and 54.9 % of Th, U and REEs respectively, contents by using the following optimum leaching conditions; Ore grain size -200 mesh; H2SO4 Concentration 20 %; agitation time 4h; Leaching temperature 75 ºC; Solid/liquid ratio (S/L) 1/2.

**Keywords:** South Eastern Part of Wadi Baroud, Uranium, REE, Thorium, Leaching.

## 1 Introduction

Uranium is the most important nuclear fuel, and it has been used to produce electricity without increasing global warming. Due to increased demand for freshwater and electrical resources, Egypt and Russia signed notices to proceed with the implementation of an intergovernmental agreement signed in 2015 between the two countries for the construction of four nuclear power plants in El Dabaa, Egypt [1].

Nuclear energy is expected to increase its global electrical production from 2.6 trillion kilowatt hours in 2008 to 4.9 trillion kilowatt hours in 2035, representing the importance of the uranium industry. The granites and related pegmatites contain the majority of radioactive occurrences in Egypt's basement rocks. The presence of accessory minerals such as zircon, monazite, thorite, uranothorite, and allanite is believed to be responsible for the high radioactivity of these rocks [2].

The dissolution of uranium from uranium-containing minerals in the ore is known as the leaching process. The physical characteristics of the ore, such as form of mineralization, ease of liberation, and the presence of other constituent minerals present, influence the choice of leaching method for dissolving uranium minerals [3].

Various types of leaching processes based on acid and alkaline leaching methods have been produced for processing uranium ore of various characteristics over the last few decades [4]. Some problems occurred during the filtration and washing of the leach slurry using the El Sella ore materials due to the relatively high presence of clayey materials. At the Inshas Pilot Plant Facility, sulfuric acid is used in the leaching process, which could result in the loss of some valuable uranium [5].

As a result, acid leaching was chosen as the appropriate technique in the current research. The valuable elements are leached using a variety of techniques in acid leaching. A side from acid leaching under pressure, these include agitation leaching, percolation leaching, hot digestion, constant pH leaching, acid curing at high solids (pugging), and constant pH leaching. For some materials, each technique has a benefit. The most commonly used method in the uranium industry is agitation leaching, which provides optimum continuity of the solid contents of the pulp with the leached liquor [6].

The primary goal of refined uranium from stream sediments is to produce uranium concentrate under certain conditions: high recovery, low production costs, and high-quality

---

[*] Corresponding author e-mail: mahmoudkhattabnma@yahoo.com

concentrate. The dissolution of uranium from uranium-containing minerals and adsorbed clays is known as the leaching process. The method for dissolving uranium minerals is determined by the ore's physical characteristics, such as the form of mineralization, ease of liberation, and the presence of other constituent minerals [7].

Uranium is a redox-sensitive element that occurs naturally in two forms U (VI) and U (IV).The redox conditions have a big effect on uranium's mobility [8].

Uranium leaching can be performed in a variety of ways, both traditional and unconventional. Acidic, alkaline, autoclave strain, heavy acid pug, and curing leaching are all examples of traditional leaching. Heap, in-situ, and bioleaching involving bacteria and fungi are examples of non-conventional leaching. In the traditional process, uranium minerals are dissolved using either acid or alkaline reagents, with sulfuric acid or sodium carbonate/sodium bicarbonate systems being the most common.

The need to develop economically viable methods in the treatment of low grade ores led to the development of non-conventional techniques using bioleaching of uranium ores. Microorganisms (bacteria and fungi) have the ability to convert solid compounds into soluble and extractable components that can then be easily retrieved. The micro-organisms do not directly attack the uranium ore during the process; instead, they create the chemical conditions that allow it to dissolve.

Kassandra et al., 2018 [9] confirmed that U enrichment levels were spread across the depth profile, not only in surface sediments but also in deep sediments; from across the North Pacific at other depths and locations, sediment redox conditions were relatively oxygen rich on the Juan de Fuca Ridge during glacial periods compared to interglacial periods. SEM-EDS and XRD analysis showed that U partitioning in the depth profile was likely affected by the dynamic interplay of leaching and precipitation cycles of U-bearing minerals. The use of Pb isotopes is as an effective method for quantitatively finger printing the origins of U-dispersal in sediment cores, as well as naturally occurring U-pollution that could become a secret geo environmental health threat.

New leaching experiments on samples representing the resulted ore material from the exploratory mining operations were required. As a result, the aim of this research was to look into the sulfuric acid leaching process of a representative sample from a new uranium occurrence in southern part of Wadi Baroud uranium ore. There is also a scarcity of data on the kinetics of uranium leaching from such ore by sulfuric acid since only a few kinetic studies have been conducted. The main goal of this study is to learn more about the kinetics of uranium dissolution in sulfuric acid solutions and how it relates to the leaching process.

## 2 Experimental

### *2.1 Geological Setting*

The southern part of Wadi Baroud is situated in Egypt's Northern Eastern Desert, about 20 kilometres west of Safaga City. The area is easily accessible through a newly built section of the Qena–Safaga asphaltic route, which runs directly to the north of the area, along W. Baroud Al Abyad. Latitudes 26$^o$ 42'54" and 26$^o$ 45'36" N, and longitudes 33$^o$ 44' 06" and 33$^o$ 47'42" E, describe the region (Figure 1).

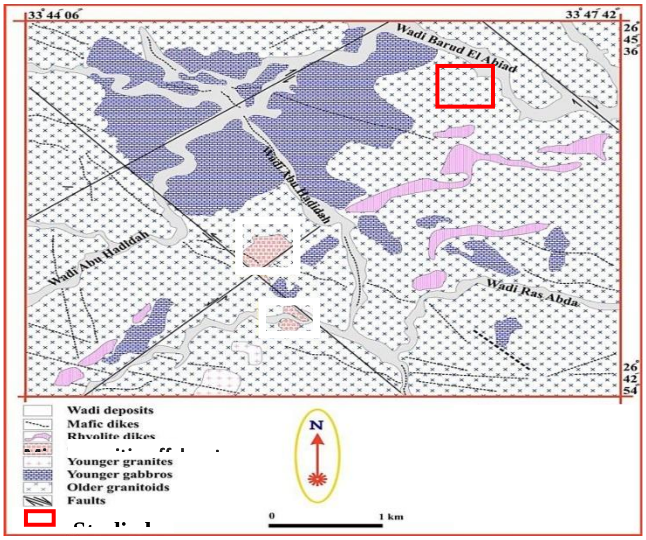

**Fig.1:** Geological map of South Eastern Part of Wadi Baroud [10].

The rock units found in the south eastern part of Wadi Baroud region can be categorized as older granites, younger gabbros, and younger granites, as well as simple and acidic dikes, in order of age. The studied region is situated south of Wadi Ras Baroud and reflects a new occurrence for radioactive mineralization in the South Eastern Part of Wadi Baroud granite.

Micro-granite offshoots intrude into older granitoids, forming younger granite. Vertical walls of micro-granite offshoots vary in length from a few meters to tens of meters, and in width from less than a meter to a few meters. These micro-granite offshoots, on the other hand, have fine to medium grain and varying degrees of coloration, such as red, pink, and reddish pink, due to the alteration processes.

In the studied region, the zone of micro-granite offshoots has the highest level of radioactivity. In the studied region, two forms of altered granites were discovered: the less altered micro-granite and the strongly altered and mineralized micro granite offshoots. The detailed sketch map of the studied region (Figure 2), on the other hand, depicts various rock unites as older granite, younger granite, and granite offshoots. Several alteration zones with distinct mineralization can be found in granite offshoots.

In the studied region, there are two types of pegmatite: the mineralized pegmatite, which is related to granite offshoots, and the natural pegmatite, which is related to normal younger granite with no evidence of mineralization [12].

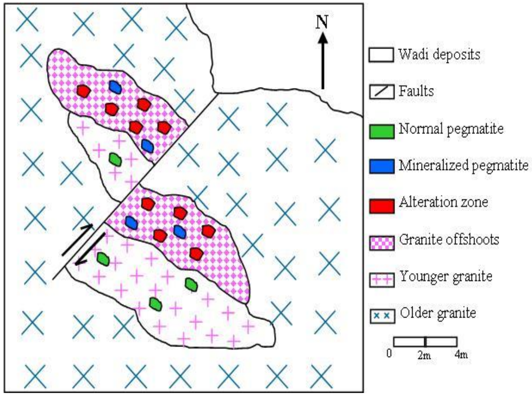

**Fig. 2:** Sketch map of the studied area.

## 2.1 Analytical Method

### 2.2.1 Mineralogical Analysis

To extract trash from the samples, they were sieved with a 2 mm sieve; then subjected to gravity separation using wiffey shaking tables. Concentrated, middling, and a rejected tailing were the fractions obtained from the shaking table separation. The composite sample concentrates were dried and prepared for heavy liquid separation with bromoform solution (specific gravity 2.811 $gcm^{-3}$). The heavy fractions that resulted from the heavy liquid separation are grouped into size fractions ranging from 1 mm to 0.063 mm.

The heavy fractions left over after bromoform separation were subjected to magnetic separation with a permanent magnet to isolate magnetite and a Frantz Isodynamic Magnetic Separator (Model L1) at 0.2, 0.5 current amperes to distinguish the minerals in magnetic sub-fractions.

Binocular Stereomicroscope was used to evaluate the sub-fractions obtained by magnetic separation. The X-ray diffraction technique (XRD) and a Philips Environmental Scanning Electron Microscope (ESEM) model XL30 were used to identify the different minerals in the studied collected samples from the Abu Hadeida region.

The heavy minerals were magnetically fractionated to make counting them under a binocular microscope easier. The heavy minerals are more concentrated in the magnetic fraction separated at 0.2 A, then the magnetic fraction separated at 0.5 A, with the nonmagnetic fractions having the lowest concentration of heavy minerals.

### 2.2.2 Determination of U, REE and Th

In the presence of diphenyl amine-4-sulfonic acid sodium salt as an indicator for uranium determination, an oximetric titration procedure against ammonium metavanedate ($NH_4VO_3$) was used [12].

Meanwhile, using Arsenazo-III as an indicator, the concentrations of REEs and Th in the resulting leach liquor were chemically calculated using the coloured process. A spectrophotometer was used to perform the coloured process [13].

Prior to titration, ammonium ferrous sulphate was used to reduce U to the correct concentration. After that, 15 percent $NaNO_2$ solution was applied until the pale brown colour disappeared, and then 20 % urea solution was added with stirring until the bubbles disappeared. 0.2 percent sodium diphenyl amine-4-sulfonic acid indicator was added to the settled solution and titrated against ($NH_4VO_3$) solution until a slightly violet red color was appeared.

### 2.2.3 Leaching Experiments

A representative sample was subjected to several agitation leaching experiments. The sample was first analyzed to determine major oxides using XRF (The Rigaku EDXRF spectrometer NEX CG, high performance SDD detector and tube power 50w = 50 kv-2mA).

Sulfuric acid was selected for the leaching process because it is a cost-effective and readily available lixiviant. A series of leaching runs with agitation were carried out. Acid concentrations and temperature are the two key factors that control the rate of uranium dissolution.

All of the leaching experiments were carried out in Teflon containers. A 10 g sample was leached with 20 mL of acid under the correct leaching conditions. The filtrate and washings were combined to create a total volume of 30 ml.

After each experiment, the residue was filtered and washed with distilled water until it was acid-free. The filtrate and washings were then calibrated to a specific volume before being checked for U, Th, and REE. The following equation (1) was used to measure the uranium leaching efficiency percent:

$$\textbf{Leaching efficiency (\%)} = C_f / C_i \, x100 \qquad (1)$$

where $C_f$ and $C_i$ are the uranium content leached out from the sample into the solution and the U content in the input ore sample respectively. Optimum conditions and selected experiments were repeated three times.

## 3 Results and Discussion

### 3.1 Mineralogical Characterization

Mineralogical investigations of southern part of Wadi Baroud microgranite revealed that the main mineral associations were enriched with many rare accessory minerals such as the euxenite-polycrase series, the columbite-tantalite series, the samarskite group, uranium-thorium minerals, rare earth minerals (cerianite), Zircon, and monazite.

#### ***Uranopyrochlore***

The average amount of Nb in the investigated pyrochlore forms was about 35.28 %, which was higher than the average content of Ta (20.03 %). At the site of A, pyrochlore forms have a high Uranium content, ranging from 12.72 to 16.49 %, with an average of 14.84 %. The compositional limits of uranopyrochlore and plumbopyrochlore minerals species were revealed by our study characterized pyrochlore species; Uranium and lead enrichment are indicated by EDAX analyses (Figure 3). XRD analysis also revealed the presence of uranmicrolite $(U, Ca)_2(Ta, Nb)_2O_6 (OH)$ (Figure 4).

### *Betafite [(U, Ca) (Nb, Ti)$_2$O$_6$]*

Betafite is a very rare mineral that can be found in the altered granites of Abu Hadeida as small anhedral grains. In addition to Ti and REE, the EDAX analysis of Betafite **(Figure 5)** reveals the existence of U and Th. X-ray diffraction (XRD) was also used to evaluate the betafite **(Figure 6)**. In South Eastern Part of Wadi Baroud granites, which resemble Betafite in composition, Nb is often replaced with Ti at the B-site.

### *Uranopilite [(UO$_2$)$_6$(SO$_4$) O$_2$ (OH)$_6$(H$_2$O)$_6$](H$_2$O)$_8$]*

For the first time in Egypt, uranopilite (a uranyl-sulfate mineral) was discovered in this analysis. It's most common in small aggregates of long prismatic crystals with a deep lemon yellow/pale greenish-yellow colour. Only because of its association with several phases of Nb-Ta mineralization does XRD accept it (Figure 7).

### *Autunite*

It is a secondary uranium mineral formed by the alteration of uraninite or pitchblende and found in the oxidation and weathering region. Autunite grains are characterized by their yellow to pale brown colour under a binocular microscope (Figure 8).

### *Zircon*

It often comes in the form of euhedral to subhedral grains in fine to very fine sizes. Prismatic to elongated grains with a good adamantine luster are popular. Bi-pyramidal termination is a characteristic of certain prismatic zircons. There are also oval, needle, spherical, and pieces. The majority of zircon grains is transparent, occasionally translucent, and range in colour from colourless to pale yellow. Zircon grains come in a variety of colours, ranging from gold to yellowish red to brown **(Figures 8 and 9)**. X-ray diffraction (XRD) was also used to assess zircon (Figures 6 and 7).

### *Uranothorite (Th, U)SiO$_4$*

Uranothorite crystals are usually transparent or opaque and range in colour from pale to dark yellow-brown. It comes in the form of granular anhedral/subhedral massive crystals with a distinctive glass or resinous shape and luster. According to EDX analysis, uranothorite contains major elements such as Th (44.86 to 54.96 wt %), Si (19.88 to 23.60 wt %), and U (44.86 to 54.96 wt %) (11.64 to 20.44 wt %). Minor quantities of Fe (1.88 to 5.68 weight %), Ca (1.09 to 2.65 weight %), and Al (2.24 to 3.95 weight %) were contained in uranothorite (Figure 8). The backscattered images revealed that uranothorite is a common component of Zircon (Figure 9).

### *Thorite, (ThSiO$_4$)*

It is one of the most common thorium silicate minerals; $ThO_2$ (49 percent to 75 %), $SiO_2$ (up to 20 %), and U (up to 10 %). Other elements such as Ca, Mg, Fe, alkalis, Ce, P, Ta, Ti, Zr, Sn, Al, Y, Pb, and $Fe^{3+}$ may be presented in small to minor amounts (Figure 9).

### *Fergusonite (YNbO$_4$)*

The fergusonite family includes REE-bearing Nb and Ta oxides, many of which are metamict and have a week's land. In contrast to other (Y,REE,U,Th)-(Nb,Ta,Ti) oxides, fergusonite (ideal formula: $YNbO_4$) is usually found as an additional material in granitic rocks and pegmatites [14,15]. On the other hand, fergusonite and other Nb-Ta-Ti oxide minerals are mostly influenced by altering chemical processes [15 and 16]. The EDAX analyses of the examined fergusonite crystals (Figure 8d) clarify that the mineral has high contents of niobium, yttrium, ytterbium, and REE elements in addition to Uranium and thorium. Fergusonite was also determined by X-ray diffraction (XRD), (Figure 6).

The chemical composition of the ore sample was listed in tableable 1. The ore sample characterized by high concentrations of U, Th, REE, Zr and Nb.

**Table 1:** Chemical composition of ore material.

| **Major Oxides** | **Conc., (%)** | **Trace Elements** | **Conc. (ppm)** |
|---|---|---|---|
| **$SiO_2$** | 69.91 | **U** | 1350 |
| **$TiO_2$** | 0.23 | **Ni** | 35 |
| **$Al_2O_3$** | 7.85 | **Co** | 85 |
| **$Fe_2O_3$** | 8.22 | **Nb** | 1200 |
| **CaO** | 0.50 | **Cu** | 38 |
| **MgO** | 0.20 | **V** | 28 |
| **MnO** | 0.18 | **Zr** | 1825 |
| **$Na_2O$** | 3.90 | **Th** | 3250 |
| **$K_2O$** | 4.70 | **REE*** | 1420 |
| **$P_2O_5$** | 1.40 | | |
| **L.O.I**<br>**Total** | 1.06<br>98.15 | | |

**Ce as reference for REE* (Marchizinco, 2000)**

**L.O.I**: loss of ignition**

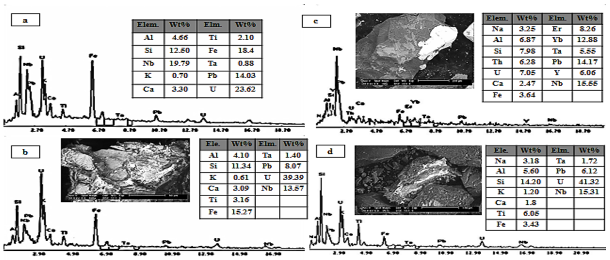

a

| Elem. | Wt% | Elm. | Wt% |
|---|---|---|---|
| Al | 4.66 | Ti | 2.10 |
| Si | 12.50 | Fe | 18.4 |
| Nb | 19.79 | Ta | 0.88 |
| K | 0.70 | Pb | 14.03 |
| Ca | 3.30 | U | 23.62 |

c

| Elem. | Wt% | Elm. | Wt% |
|---|---|---|---|
| Na | 3.25 | Er | 8.26 |
| Al | 6.87 | Yb | 12.88 |
| Si | 7.98 | Ta | 5.55 |
| Th | 6.28 | Pb | 14.17 |
| U | 7.05 | Y | 6.06 |
| Ca | 2.47 | Nb | 15.55 |
| Fe | 3.64 | | |

b

| Ele. | Wt% | Elm. | Wt% |
|---|---|---|---|
| Al | 4.10 | Ta | 1.40 |
| Si | 11.34 | Pb | 8.07 |
| K | 0.61 | U | 39.39 |
| Ca | 3.09 | Nb | 13.57 |
| Ti | 3.16 | | |
| Fe | 15.27 | | |

d

| Ele. | Wt% | Elm. | Wt% |
|---|---|---|---|
| Na | 3.18 | Ta | 1.72 |
| Al | 5.60 | Pb | 6.12 |
| Si | 14.20 | U | 41.32 |
| K | 1.20 | Nb | 15.31 |
| Ca | 1.8 | | |
| Ti | 6.05 | | |
| Fe | 3.43 | | |

**Fig.3:** EDX mineral analysis and BSE of: a,b, d- uranopyrochlore c- plumbopyrochlore.

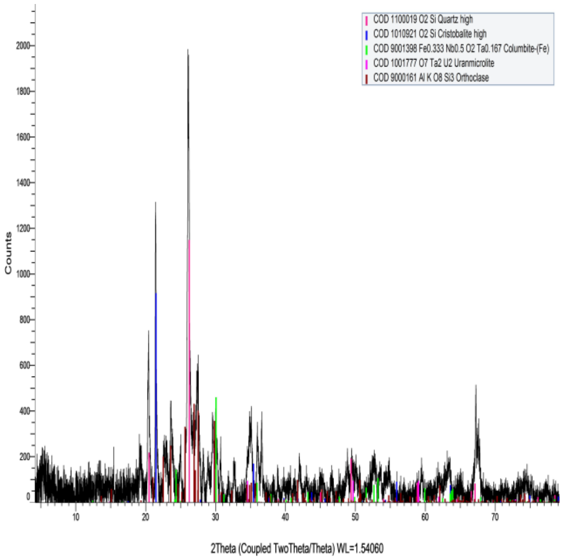

**Fig.4:**X-ray diffraction pattern of uranomicrolite, columbite.

| Ele. | Wt% | Elm. | Wt% |
|---|---|---|---|
| **Al** | 6.23 | **Er** | 7.59 |
| **Si** | 3.19 | **Yb** | 15.64 |
| **Th** | 9.63 | **Ta** | 4.07 |
| **Ca** | 2.23 | **U** | 6.32 |
| **Ti** | 22.30 | **Y** | 7.23 |
| **Fe** | 2.82 | **Nb** | 11.40 |
| **Mn** | 1.34 | | |

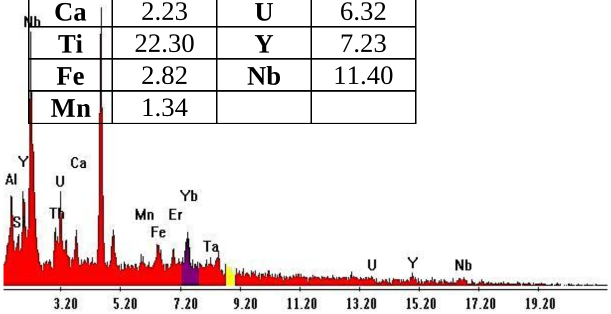

**Fig. 5:** EDX mineral analysis and BSE of betafite.

Temperature variation can cause slowness of completing a paper on word, using an air conditional or a fan is recommended.

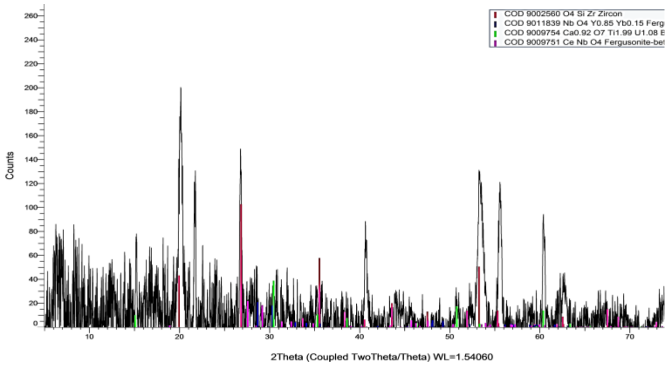

**Fig.6:** X-ray diffraction pattern of zircon, fergusonite and betafite.

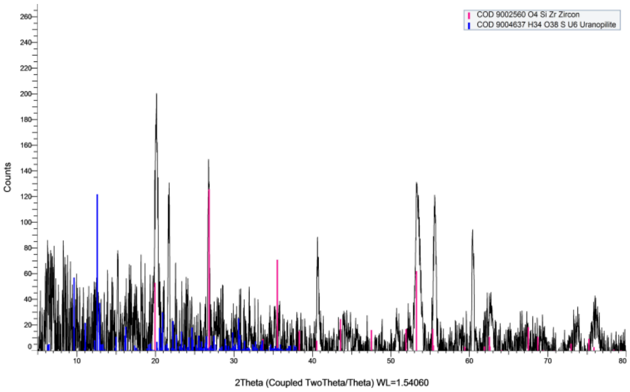

**Fig. 7:** X-ray diffraction pattern of uranopilite-zircon.

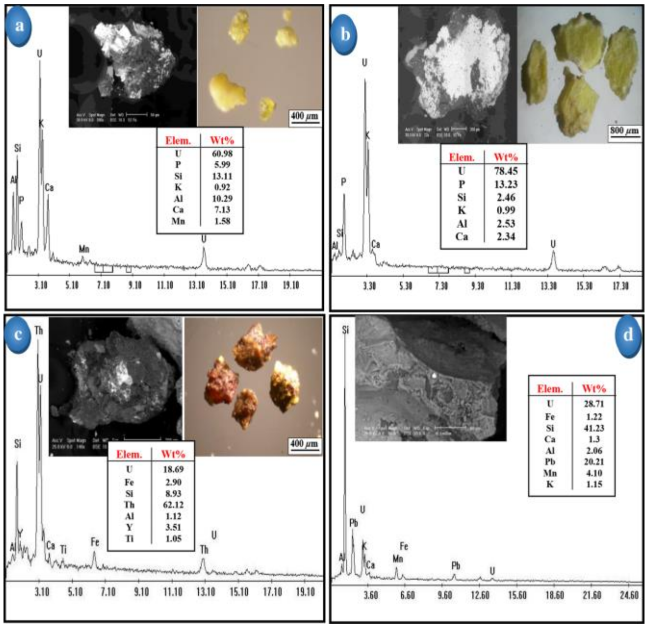

a

| Elem. | Wt% |
|---|---|
| U | 60.98 |
| P | 5.99 |
| Si | 13.11 |
| K | 0.92 |
| Al | 10.29 |
| Ca | 7.13 |
| Mn | 1.58 |

b

| Elem. | Wt% |
|---|---|
| U | 78.45 |
| P | 13.23 |
| Si | 2.46 |
| K | 0.99 |
| Al | 2.53 |
| Ca | 2.34 |

c

| Elem. | Wt% |
|---|---|
| U | 18.69 |
| Fe | 2.90 |
| Si | 8.93 |
| Th | 62.12 |
| Al | 1.12 |
| Y | 3.51 |
| Ti | 1.05 |

d

| Elem. | Wt% |
|---|---|
| U | 28.71 |
| Fe | 1.22 |
| Si | 41.23 |
| Ca | 1.3 |
| Al | 2.06 |
| Pb | 20.21 |
| Mn | 4.10 |
| K | 1.15 |

**Fig.8.a,b;** BSE binocular images and EDX analyses of autunite. c; BSE, binocular images and EDX analyses of uranothorite. d; EDX mineral analysis and BSE of fergusonite.

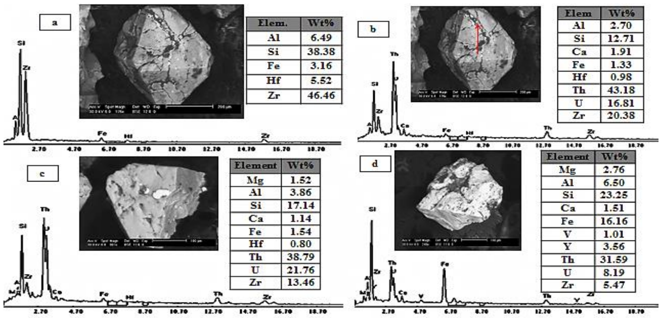

a

| Elem. | Wt% |
|---|---|
| Al | 6.49 |
| Si | 38.38 |
| Fe | 3.16 |
| Hf | 5.52 |
| Zr | 46.46 |

b

| Elem | Wt% |
|---|---|
| Al | 2.70 |
| Si | 12.71 |
| Ca | 1.91 |
| Fe | 1.33 |
| Hf | 0.98 |
| Th | 43.18 |
| U | 16.81 |
| Zr | 20.38 |

c

| Element | Wt% |
|---|---|
| Mg | 1.52 |
| Al | 3.86 |
| Si | 17.14 |
| Ca | 1.14 |
| Fe | 1.54 |
| Hf | 0.80 |
| Th | 38.79 |
| U | 21.76 |
| Zr | 13.46 |

d

| Element | Wt% |
|---|---|
| Mg | 2.76 |
| Al | 6.50 |
| Si | 23.25 |
| Ca | 1.51 |
| Fe | 16.16 |
| V | 1.01 |
| Y | 3.56 |
| Th | 31.59 |
| U | 8.19 |
| Zr | 5.47 |

**Fig. 9.a;** BSE binocular images and EDX analyses of metamict zircon. b; BSE, binocular images and EDX analyses of uranothorite as fissure filling in zircon. c; BSE, images and EDX analyses showing uranothorite as inclusion in zircon. d; BSE binocular images and EDX analyses of thorite with V, Y, Zr.

### *3.2 Effect of different concentrations of leaching agent ($H_2SO_4$)*

This factor has been studied by applying different acid concentrations, 10 g of the stream sediment sample, 20 ml of leaching agent ($H_2SO_4$) with concentration ranging from 5 % to 25 %, and then the agitation done for 2 hours at room temperature, where other factors have been fixed **(Figure 10)**.

Obviously it was found that leaching percent of uranium was increased gradually with increasing $H_2SO_4$ concentration from 5 % to 25 %. After that the leaching concentration was decreased. Probably due to increase in re-precipitation of uranium, so this occurs in sulfate media due to the equilibration between $HSO_4^-$, $SO_4^{2-}$ and $H_2SO_4$ due to hydrolysis.

Table 2 Indicates why the row corresponding to 20 % concentration is in bold because it is the optimum condition for leaching U and Th without consuming more acids which considered favorite for economy.

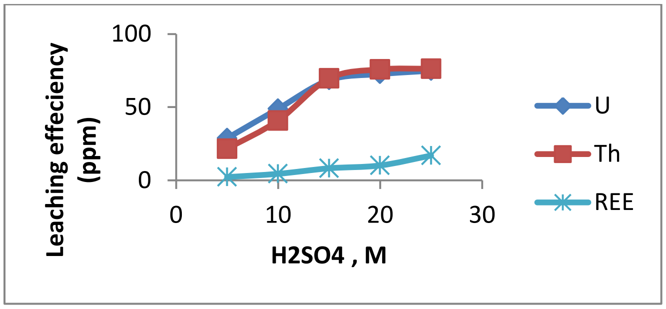

**Fig. 10:**The effect of different concentration of $H_2SO_4$ on the leaching of U, Th and REE.

**Table 2:** Dissolution Efficiency of U, Th, REE, Nb and Zr using different concentration of $H_2SO_4$.

| **$H_2SO_4$ Concentration (%)** | **Dissolution Efficiency (%)** | | |
|---|---|---|---|
| | **U** | **Th** | **REE** |
| 5 | 28.8 | 21.65 | 2.3 |
| 10 | 48.9 | 40.9 | 4.53 |
| 15 | 68.5 | 69.6 | 8.3 |
| **20** | **72.6** | **75.8** | **10.23** |
| 25 | 74.9 | 76.3 | 16.98 |

### *3.3 Effect of solid/liquid ratio (S/L)*

The effect of S/L ratio upon U, REE and Th leaching efficiencies of the study ore material was studied in the range of 1/2 to 1/5 using 20 % $H_2SO_4$ on -200 mesh size ore, for 2 h as agitation time at room temperature **(Figure 11a)**.

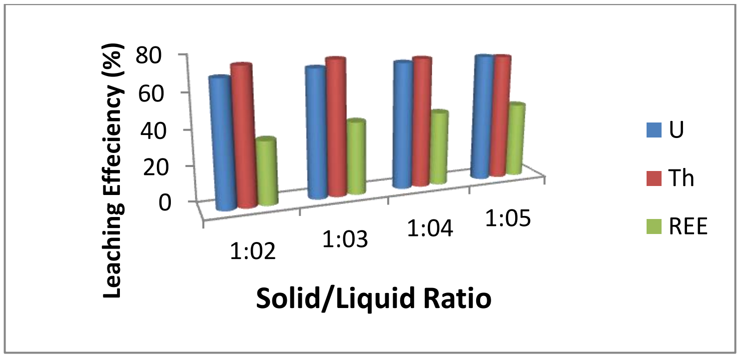

**Fig. 11a:** The effect of solid/liquid ratio on the leaching of U, REE and Th.

Also the effect of agitation time upon U, REEs and Th leaching efficiencies of the study ore material was studied in the range of 1 h to 5 h using 20 % $H_2SO_4$ on -200 mesh size ore and 1/2 S/L ratio at room temperature **(Figure 11b)**.

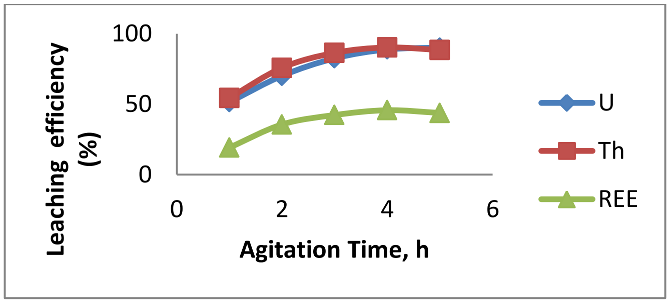

**Fig.11b:** The effect of Agitation time ratio on the leaching of U, REE and Th.

### *3.4 Effect of Leaching Temperature*

The effect of leaching temperature upon U, REEs and Th leaching efficiencies of the study ore material was studied in the range of room temperature to 95 ºC using 20 % $H_2SO_4$ on -200 mesh size ore and 1/2 S/L ratio and agitation time 4 h (Figure 12).

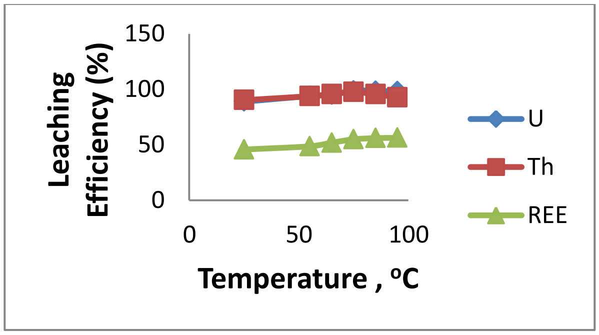

**Fig. 12:** effect of temperature on the leaching of U, REE and Th.

The leaching efficiency of Th decreases as the leaching temperature increases up to 85 °C. This is due to the re-precipitation of thorium sulfate upon elevating the temperature of the solution into the neighborhood of its boiling point [17].

From the acidic atmospheric agitation leaching study upon the dissolution of U, Th and REEs from the study ore material, it can be concluded that this leaching method is satisfactory in dissolving 97.6 %, 98.8 % and 54.9 % of Th, U and REEs respectively, contents by using the following optimum leaching conditions; Ore grain size -200 mesh; $H_2SO_4$ Concentration 20 %; agitation time 4 h; Leaching temperature 75 ºC and Solid/liquid ratio 1/2.

Applying the previous optimum leaching conditions upon the study raw material would separate both of U, Th and apart of REEs from Nb, and Zr which are left behind in the residue. After filtration and washing, the total volume of the obtained sulfate leach liquor was adjusted to be 2.5 L $kg^{-1}$ ore and its pH was found to attain 0.8- 0.9. The prepared sulfate leach liquor was found to assay 1.26 g $L^{-1}$ of Th 0.533 g $L^{-1}$ of U, 0.27 g $L^{-1}$ of REEs and 20.19 g $L^{-1}$ of Fe.

It is customary to regard the form of the resulting uranium in solution as being $UO_2SO_4$. In practice, however high proportions of the anionic complexes $UO_2\,(SO_4)_2^{2-}$ and $UO_2(SO_4)_2^{4-}$ are also present. As a matter of fact, the dissolved uranium occurs in all three forms simultaneously, the abundance of which being controlled by complex equilibrium involving the concentrations of $H^+$, $SO_4^-$ and $HSO_4^-$ ions besides that of the various forms of dissolved uranium [18]. These complex anionic forms take a major role in the subsequent purification and recovery of uranium from the pregnant acid liquor that is quite rich in co-dissolved impurities incorporated in the ore. That is why these complex forms are quite responsible for the importance of sulfuric acid in uranium leaching.

$$\mathbf{UO_3 + H_2SO_4 \longrightarrow UO_2SO_4 + H_2O} \qquad (1)$$

$$\mathbf{UO_2 + Fe_2(SO_4)_3 \longrightarrow UO_2SO_4 + 2\,FeSO_4} \qquad (2)$$

$$\mathbf{UO_2SO_4 \rightleftarrows UO_2^{2+} + SO_4^{2-}} \qquad (3)$$

$$\mathbf{UO_2^{2+} + 2SO_4^{2-} \leftrightarrows UO_2\,(SO_4)_2^{2-}} \qquad (4)$$

$$\mathbf{UO_2\,(SO_4)_2^{2-} + SO_4^{2-} \longrightarrow UO_2\,(SO_4)_3^{4-}} \qquad (5)$$

The re-precipitation of uranium is due to sulfate speciation with respect to leaching decrease. This may be due to precipitation of some dissolved constituents which might be associated with some uranium. Jarosite, $KFe_3(OH)_6(SO_4)_2$ or else lepidocrocite, 4FeO(OH) might be formed and precipitated in association with some uranium [19].

It is shown from the effect of temperature on the leachability of uranium from the present study that there is an increase of uranium leachability with temperature and the stream sediment minerals should be subjected to 80 ºC in order to be amenable to leaching, this is quite logic since the rate of most chemical reactions various exponentially with the reciprocal of the absolute temperature according to Arrhenius equation [20].

$$\mathbf{dc/dt = -\,K\,exp\,(-E_a/RT)} \qquad (6)$$

where dc/dt is the rate of leaching reaction; K. is the pre-exponential factor; $E_a$ is the energy of activation; R is the gas constant and T is the absolute température.

Kinetic expressions are widely used to develop an understanding of the reaction mechanism for hydrometallurgical processes which can be described as the heterogeneous reaction;

$$\mathbf{A_{(aq)} + bB_{(S)} \longrightarrow Products} \qquad (7)$$

The percent uranium dissolution can be converted to a fraction of the uranium reacted (X) and applied to the three common kinetic models listed below. This was utilized in the present study assuming the following principles;

$$\mathbf{X = \%\ uranium\ extraction/100} \qquad (8)$$

a) The shrinking core model (controlled by diffusion through an inert layer)

$$\mathbf{K_{ap}t = 1\text{-}3\,(1\text{-}X)^{2/3} + 2\,(1\text{-}X)} \qquad (9)$$

b) The shrinking sphere model (chemical reaction controlled process)

$$\mathbf{K_{ap}t = 1\text{-}\,(1\text{-}X)^{1/3}} \qquad (10)$$

c) The shrinking sphere model (diffusion controlled process)

$$\mathbf{K_{ap}t = 1\text{-}\,(1\text{-}X)^{2/3}} \qquad (11)$$

where $k_{ap}t$ is the apparent rate constant and t is the time in seconds

The shrinking core model is an idealized kinetic model commonly used in hydrometallurgical applications to model various leaching systems [21]. The shrinking sphere reaction controlled model applies in situations where the rate of the leaching reaction is not hindered by the effects of mass transport. As the flux of reactants towards or away from the particle surface is mass transport restricted, a diffuse layer forms at the particle's surface, and the leaching process is said to follow the shrinking sphere diffusion regulated model [22].

## 4 Conclusions

Mineralogical investigations of Gabal Abu Hadeida microgranite revealed that the main mineral associations were represented by uranium, thorium and REEs-minerals (thorite, uranothorite, zircon, xenotime and monazite), REE-bearing minerals (cerianite), Nb-Ta minerals (columbite, ferrocolumbite and yttro-columbite) and base metals included (pyrite, chalcopyrite, arsenopyrite and sphalerite) in addition to apatite, titanite, cassiterite, epidote, garnet and iron oxides. The average $SiO_2$ content was 68.91 %, the average $Al_2O_3$ content was 7.85 % and the average $Fe_2O_3$ content was 8.22 %. The following are the average contents of the minor constituents: CaO+MgO were 0.70 %, $Na_2O+K_2O$ were 8.6 %, $P_2O_5$ was 1.4 % and LOI was 1.6 %. The concentration of U, Th, Zr and Nb were 1350, 3250, 1825 and 1200 ppm respectively. it can be concluded that this leaching method is satisfactory in dissolving 97.6 %, 98.8 % and 54.9 % of Th, U and REEs respectively, contents by using the following optimum leaching conditions; Ore grain size -200 mesh; $H_2SO_4$ Concentration 20 %; agitation time 4h; Leaching temperature 75 ºC; Solid/liquid ratio 1/2.

## References

[1] Budnitz, R. J, Rogner H. H., Shihab-Eldin, A. Expansion of nuclear power technology to new countries-SMRs, safety culture issues, and the need for an improved international safety regime. Energy Policy 119:535-544 (2018). doi:org/10.1016/j. enpol.2018.04.051

[2] Schurmann, H M. The Precambrian along the Gulf of Suez and the northern part of the Red Sea. E.J. Bill, Netherland., **404** (1966)

[3] Merritt, R. C. In: The Extractive Metallurgy of Uranium, Colorado, School of Mines Res. Inst., Golden, Colorado., **83** (1971).

[4] Gupta, C. K., and Mukherjee, T. K. Hydro-metallurgy in Extraction Processes. CRC Press, Boca Raton, I, 70 (1990). doi: 10.1201/9780203751404

[5] Khawassek, Y.M. Uranium Recovery from Inshas Pilot Plant Unit from El Sela Shear Zone, South Eastern Desert, Egypt. Nuclear Sciences Scientific Journal., **3(1)**, 169-179, (2011) doi: 10.21608/nssj.2014.30972.

[6] Zou Y, Liu Y, Wang X, Sheng G, Wang S, Ai Y, Ji Y, Liu Y, Hayat T, Wang X. Glycerol-modified binary layered double hydroxide nanocomposites for uranium immobilization via extended X-ray absorption fine structure technique and density functional theory calculation. ACS Sustainable Chemistry and Engineering., **5(4)**, 3583-3595 (2017).

[7] Bayramoglu, G, Arica M. Y. Polyethylenimine and tris (2-aminoethyl) amine modified p (GA–EGMA) microbeads for sorption of uranium ions: equilibrium, kinetic and thermodynamic studies. Journal of Radioanalytical and Nuclear Chemistry. May1; **312(2)**,293-303(2017). doi; 10.1007/s10967-017-5216-z

[8] Liu J, Luo X, Wang J, Xiao T, Yin M, Belshaw NS, Lippold H, Kong L, Xiao E, Bao ZA, Li N. Provenance of uranium in a sediment core from a natural reservoir, South China: Application of Pb stable isotope analysis. Chemosphere, 1; **193**,1172-1180(2018). doi; 10.1016/j.chemosphere.2017.11.131

[9] Kassandra M. Costa, Robert F. Anderson, Jerry F. McManus, Gisela Winckler, Jennifer L.Middleton, Charles H. Langmuir. Trace element (Mn, Zn, Ni, V) and authigenic uranium (aU) geochemistry reveal sedimentary redox history on the Juan de Fuca Ridge, North Pacific Ocean. Geochimica et CosmochimicaActa.,**236(1)**,79-98(2018). doi.org/10.1016/j.gca.2018.02.016

[10] Omran A A. Geology, mineralogy and radioelements potentiality of microgranite dikes to the South of wadi Abu Hadeida area, Northern Eastern Desert, Egypt. Al Azhar Bulletine of Science., **25**, 47-62 (2014).

[11] Abd El Monsif, M. Geochemistry and Radioactive Mineralization Inspections of the Pegmatite Bodies Associating Variable Granitic Environs, Abu Hadeida Area, North Eastern Desert, Egypt. Journal of Basic and Environmental Sciences, ISSN 2356-6388, 2536-9202,, **8**, 1-14 (2021).

[12] Mathew, K.J., Burger, S., Ogt, S.V., Mason, P.M. and Narayanan, U.I. Uranium assay determination using Davies and Gray titration. Processing the Eighth International Conference on Methods and Applications of Radioanalytical Chemistry (Marc Viii) Kaailua-Kona, Hawaii, 5 (2009)

[13] Marczenko, Z. Spectrophotometric determination of elements, John Wiley and Sons, Harwood, New York. ISBN: 978-0-444-50524-8 (2000).

[14] Poitrasson, F., Paquette, J.L., Montel, J.M., Pin, C., Duthou, J.L. Importance of late-magmatic and hydrothermal fluids on the Sm-Nd isotope mineral systematics of hypersolvus granites. Chem. Geol., **146**, 187–203. doi; 1016/S0009-2541(98)00010-2 (1998).

[15] Ercit, T.S. Identification and alteration trends of granitic-pegmatite-hosted (Y,REE,U,Th)-(Nb,Ta,Ti) oxide minerals: A statistical approach. Can. Mineral., **43**, 1291-1303 (2005) doi: 10.2113/gscanmin.43.4.1291

[16] Ewing, R.C. The crystal chemistry of complex niobium and tantalum oxides. IV. The metamict state: Discussion. Am. Mineral., **60**, 728-733 (1975).

[17] Lewis, C.J. and Edward, L.C. Thorium recovery process, US Patent., **2(993)**,752. US63012956A (1961).

[18] Mcquiston, F.W., Jr. Properties of gold ores and recovery methods: in SME Mineral Processing Handbook, published by the Society of Mining Engineers, N.L. Weiss, Editor. doi; 10.1007/978-3-642-77184-2 (1985)

[19] Amer, T.E, EL-Hazek, M.N., Abdel Fattah, N.A. El-Shamy, A.S., Abdellah, W.M., EL-Shahat, M.F. Processing of Abu Zeneima Mineralized Gibbsite Ore Material For The Recovery of Aluminium, Zinc and Individual Light Rare Earth Oxides. Isotope and Radiation Research., **41**,1163-1177.

[20] HA Awad, HMH Zakaly, AV Nastavkin and Atef El-Taher., Radioactive content in the investigated granites by geochemical analyses and radiophysical methods around Um Taghir, Central Eastern Desert, Egypt. Journal of Physics: Conference Series **1582 (1)**, 012007 (2020).

[21] Gbor, P., Jia, C. Critical evaluation of coupling particle size distribution with the shrinking core model. Chemical Engineering Science. Elsevier., **59**,1979-1987(2004). doi 10.1016/j.ces.2004.01.047.

[22] Levenspiel, O. Chemical reaction engineering. 3rd edition. Wiley, New York. doi; 10.1021/ie990488g (1999).